



UTRECHT UNIVERSITY

DEBYE INSTITUTE

BACHELOR THESIS

Temperature measurements in an optical dipole trap

Author:
G.W.H. VAN DEN
HENDEL

Supervisors:
Dr. D. VAN OOSTEN
S. PRATAMA MSc.
B. O. MUSSMANN Msc.

February 15, 2014

Contents

1	Introduction	2
2	Theory	3
2.1	Magneto-Optical Trap	3
2.1.1	Velocity dependent force	3
2.1.2	Position dependent force	6
2.2	Optical Dipole Trap	10
2.3	Density distribution	13
3	Experiment	15
3.1	Experimental setup	15
3.1.1	Compartments	16
3.1.2	Optical dipole trap	18
3.2	Imaging	19
4	Results	21
4.1	Column number density	21
4.2	Data fitting	23
4.3	Temperature	26
5	Conclusion	30
6	Acknowledgements	31
7	A Rubidium hyperfine structure	32

1 Introduction

In the field of cold atom nanophotonics, the interaction between atoms and photons is studied. In our research group, we bring ^{87}Rb atoms close towards a golden sample surface to study the interactions between these atoms and nanostructures on the sample. From a Rubidium source, atoms are trapped in a 2D magneto-optical trap (MOT). From here, atoms are pushed towards a vacuum chamber by an on-resonance beam, where they are trapped in a 3D-MOT. By overlapping an optical dipole trap (ODT) with the cloud of atoms in the 3D-MOT, the atoms are loaded in the ODT and can be transported to an optical conveyor. This conveyor will then transport the atoms to the golden sample surface.

In order to successfully transport the atoms, it is important to study the characteristics of the atoms while they are in the ODT. In this theses, the relation between the temperature and the time the atoms are trapped in the ODT is studied. The temperature is related to the spatial distribution of the atoms. By measuring the spatial distribution using absorption imaging, we determine the temperature in the ODT.

2 Theory

The goal of this experiment is to perform temperature measurements on a cloud of atoms in an ODT. Trap depths are generally below 1 mK, so the atoms first need to be cooled down to the μK regime. The ODT is loaded by overlapping the beam with the atom cloud in the 3D-MOT. More atoms can be trapped if the density of the cloud is high. A common way to obtain a cold dense cloud of atoms is by using a magneto-optical trap (MOT). A brief theoretical description of the MOT is given in section (2.1). After the atoms are cooled down, they are loaded in the ODT. The theory of optical dipole trapping and the potential of the trap are discussed in section (2.2). In section (2.3) a theoretical description of the density distribution of the atoms in the trap is given.

2.1 Magneto-Optical Trap

To obtain a cold dense cloud of atoms, the MOT applies two different forces. It applies a velocity-dependent force to slow the atoms down and a position-dependent force to confine them to a small region of space. This section consists of two parts describing each of the forces in the MOT. The velocity-dependent force is discussed in section (2.2.1) and the position-dependent force in section (2.2.2).

2.1.1 Velocity dependent force

The velocity of the atoms is reduced by applying an optical force on them. This is done by directing a laser beam at atomic resonance frequency ω_0 towards the atoms. The atoms will absorb the photons and go to the excited state. During this collision, the atom absorbs the momentum of the photon $p = \hbar k$. Atoms moving in the opposite (same) direction of the beam will therefore have their momentum reduced (increased) by a factor of $p = \hbar k$. Once the atom is in the excited state, it will eventually fall back into its ground state due to spontaneous emission. The atom will re-emit the photon in a random direction. Since this direction is random, the average momentum gain is the same in all directions after many such events. Therefore, the net force from the spontaneous emission is zero. The momentum of the atoms can be reduced by making them only absorb photons when they are moving into the beam. This can be realized by exploiting the Doppler effect.

Doppler cooling

When an atom is moving at a certain velocity, the frequency of a laser beam in the atom's frame of reference is shifted due to the Doppler shift. An atom moving towards the beam with velocity \vec{v} will see the laser's frequency ω_L shifted at $\omega'_L = \omega_L - \omega_D$, with $\omega_D = -\vec{k} \cdot \vec{v}$, the Doppler shift. In the case when the atom is moving towards the beam, \vec{k} and \vec{v} are opposite in sign, so the Doppler shift

is positive. If the frequency of the photon in the atom's frame of reference is close to its resonance frequency ω_0 , there is a high probability that the atom will absorb the photon. To realize this, the frequency of the laser is lowered by an amount equal to the Doppler shift. This lowering of frequency and the Doppler shift then cancel each other out, so the atom moving towards the beam sees the beam at resonance. The changing of the frequency is called the detuning of the laser and is written as

$$\delta = \omega_L - \omega_0 \quad (1)$$

Here, ω_L is the frequency of the laser and ω_0 the resonance frequency of the atom. We say that the laser is red detuned if $\delta < 0$ and blue detuned if $\delta > 0$. By red-detuning the laser, we obtain a high absorption probability when an atom is moving into the beam and a low absorption probability when an atom is moving away from the beam. This is because atoms moving away from the beam will see the lasers frequency to be even further shifted away from resonance. Hence, absorption and re-emission will result in momentum loss and the atoms are cooled. This momentum transfer can be quantified in the following way. As stated before, the momentum of an atom is reduced by $p = \hbar k$, each time it absorbs a photon. If we know the scattering rate, which is the number of momentum transfers per unit of time, then the force is given by the momentum change per scattering event times the scattering rate. This gives

$$\vec{F} = \hbar \vec{k} \gamma_p \quad (2)$$

where γ_p denotes the scattering rate. The scattering rate is given by [2]

$$\gamma_p = \left(\frac{\gamma}{2}\right) \frac{s_0}{1 + s_0 + 4(\Delta/\gamma)^2} \quad (3)$$

Here γ denotes the natural line width, $s_0 = I/I_{sat}$ is the ratio between the intensity of the beam, $I_0 = \pi \hbar c / 3 \lambda^3 \tau$ the saturation intensity, $\tau = 1/\gamma$ the lifetime of the excited state and $\Delta = \delta - \omega_D$. From this equation we can see that, for a given s_0 , maximum scattering occurs when $\Delta = 0$ or $\delta = \omega_D$. This means that the detuning needs to be equal to the Doppler shift, so the atoms see the laser beam at resonance. The scattering rate can also be increased by increasing the intensity of the beam. For high intensities $I \gg I_{sat}$, the factor s_0 becomes much bigger than $(\Delta/\gamma)^2$. This gives a maximum scattering rate of $\gamma/2$ and the maximum scattering force

$$\vec{F} = \frac{\hbar k \gamma}{2}. \quad (4)$$

Therefore, the cooling is most efficient if high intensities are used.

Optical molasses

Up to this point, only the interaction of atoms with a single laser beam has been discussed. Eventually, atoms moving in any direction need to be cooled. For this, two counter propagating beams are placed in every spatial direction. This makes a total of six beams that reduce every spatial component of the velocity. The overlapping volume of these beams is called an optical molasses. Let us first consider the one dimensional case where an atom is moving along the x -axis. Two counter propagating beams are placed along this axis. Since the atom experiences a different Doppler shift from the two beams, the force from each beam will be different. This has to be taken into account in equation (2) for the scattering force. Doing this, the scattering force becomes

$$F_{\pm} = \pm \frac{\hbar \vec{k} \gamma}{2} \frac{s_0}{1 + s_0 + 4(\Delta_{\pm}/\gamma)^2} \quad (5)$$

with $\Delta_{\pm} = \delta \mp |\omega_D|$. The total force on the atom in the optical molasses is the sum of these forces.

$$F_{OM} = F_+ + F_- = \frac{\hbar \vec{k} \gamma s_0}{2} \left(\frac{1}{1 + s_0 + 4(\Delta_+/\gamma)^2} - \frac{1}{1 + s_0 + 4(\Delta_-/\gamma)^2} \right) \quad (6)$$

For small Doppler shifts, $|\vec{v}| \ll |\gamma/k$, the sum of these forces can be linearly approximated. By making a linear approximation, the force the atom experiences in the optical molasses is then given by [2]

$$F_{OM} \simeq \left(\frac{8\hbar k^2 \delta}{\gamma} \frac{s_0}{[1 + s_0 + 4(\delta/\gamma)^2]^2} \right) \vec{v} = \beta \vec{v} \quad (7)$$

Reading from this equation, the velocity of the atom could eventually be reduced to zero and the atom cloud would reach a temperature of 0 K. Heating mechanisms will prevent this from happening. When the atoms absorb and re-emit photons, the re-emitting causes some recoil in a random direction. This gives a small contribution in kinetic energy which heats the sample of atoms. The minimum temperature that can be obtained is when the cooling and heating mechanisms are in equilibrium and is called the Doppler cooling limit [4]

$$T_D = \frac{\hbar \gamma}{2k_B}. \quad (8)$$

For ^{87}Rb , this temperature is $145.57 \mu\text{K}$ [4].

By applying a velocity-dependent force, the atoms can be cooled, but they are not trapped in space. By introducing an inhomogeneous magnetic field, the Zeeman shift can be exploited. This will be discussed in the next section (2.1.2).

2.1.2 Position dependent force

For optimal loading of the ODT, we want the atom cloud to be dense. This can be done by applying a position dependent force on the atoms. The force can be made such that when an atom is moving away from the centre, it will be pushed back to the centre. This can be realized with the right choice of polarization and positioning of the beams.

For a two level atom with a ground state $F = 0$ and an excited state $F = 1$, the energy levels of the excited state are split into three components: $m_f = 0, \pm 1$. Because of the selection rules, different energy states are excited by different types of polarized light. The $m_f = -1$ state is excited by left handed circular polarized light (σ^-) and the $m_f = +1$ state by right handed circular polarized light (σ^+). This is represented in figure (1).

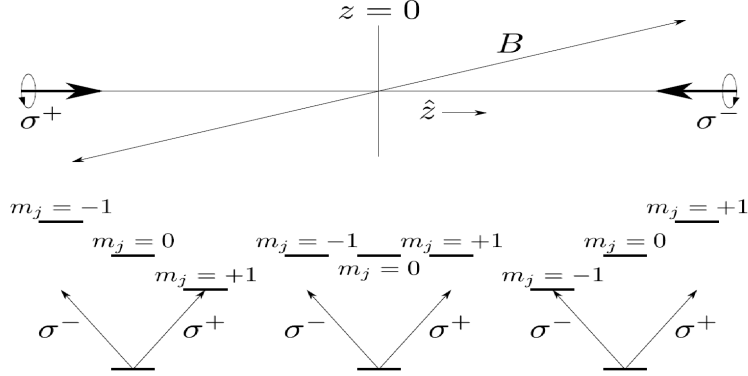


Figure 1: Energys states in different regimes of the magnetic field. Different types of light polarization excite different energy levels, as indicated

Let us now apply a linearly inhomogeneous magnetic field $\vec{B}(z) = \alpha z$. In the region $z > 0$ the magnetic field $B > 0$. In this region, the $m_f = +1$ state is shifted up and the $m_f = -1$ state is shifted down. In the $z < 0$ regime, the more the atom moves to the right, the more the $m_f = -1$ state is shifted down. Eventually the energy state is shifted down far enough for the atom to see it on resonance. This can also be seen as the point where the lines cross in figure (2). This is only the case when the beam on the right is left handed circular polarized, because only this light can excite the $m_f = -1$ energy state. Therefore, the beam coming from the right is given this polarization. In the $z > 0$ region, atoms that are moving to the right have a higher collision rate with the beam coming from the right than with the beam coming from the left.

Hence, the net force on the atom will be in the $-z$ -direction, which is the direction of the centre of the trap. For the $z < 0$ regime, the magnetic field $B < 0$ and the $m_f = +1$ energy state is shifted down. With the same reasoning as in the $z > 0$ regime, the beam coming from the left is given a right handed circular polarization.

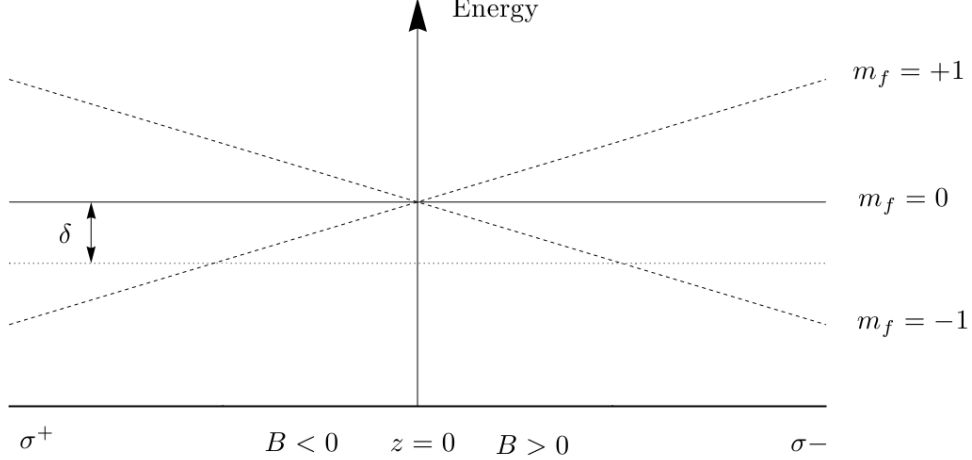


Figure 2: The energy levels of different states. The horizontal line is the energy of the laser beam. When this line crosses one of the energy states of the atom, the atom will see the beam at resonance.

Taking the Zeeman shift into account, the force on the atom in the optical molasses becomes [1]

$$F_{\pm} = \pm \frac{\hbar k \gamma}{2} \frac{s_0}{1 + s_0 + 4(\Delta_{\pm}/\gamma)^2} \quad (9)$$

where $\Delta_{\pm} = \delta \mp \omega_D \pm \omega_Z$ and $\omega_Z \sim B$.

So far, a theoretical description of the MOT and the forces on the atoms has been discussed. Once the atoms are trapped in the 3D-MOT, they are loaded in the ODT. A theoretical description of the optical dipole trap is given in section (2.2).

2.2 Optical Dipole Trap

The optical dipole trap (ODT) will transport the atoms towards the optical conveyor. This conveyor will then transport the atoms towards the sample surface. In this section, a theoretical description of the optical dipole trap is given. Here we will derive the potential in of the trap that is needed to find the density distribution.

The simplest form of an ODT is a focused beam trap and consists of a single Gaussian beam. The intensity distribution of a Gaussian beam is given by [6]

$$I(r, \omega) = I_0 \exp\left(\frac{-2r^2}{\omega(z)^2}\right). \quad (10)$$

Here, I_0 is the intensity at the focus and is obtained by dividing the power P of the laser by the area at the focus. This gives $I_0 = 2P/(\pi\omega_0^2)$. Furthermore, $\omega(z)$ is the beam waist where the intensity has dropped to $1/e^2$. The term $\omega(z)$ depends on the spatial coordinate z and is given by

$$\omega(z) = \omega_0 \sqrt{1 + (z/z_R)^2}, \quad z_R = \eta\pi\omega_0^2/\lambda \quad (11)$$

Here, z_R is the Rayleigh range, which is the depth of focus when focusing a Gaussian beam. The term ω_0 is the minimum beam waist. Equation (10) gives the intensity distribution for a circular Gaussian beam. For an elliptical beam, the radial beam waist ω_r is split into two components, ω_x and ω_y for the beam waists in the x -, and y -direction. This means we have to change the intensity distribution by taking these beam waists into account. For the intensity distribution for an elliptical beam we have

$$I(r, \omega) = I_0 \exp\left(\frac{-2x^2}{\omega_x^2(z)} + \frac{-2y^2}{\omega_y^2(z)}\right) \quad (12)$$

The intensity at the focus is now obtained in a similar way as before, but now we divide the power by the area of the elliptical beam at the focus. This gives $I_0 = (2P)/(\pi\omega_{x,0}\omega_{y,0})$.

The electric field of the beam induces an atomic dipole moment. To find the relation between the electric field and the atomic dipole moment, we consider the atom in Lorentz's model of a classical oscillator. In this model, an electron is elastically bound to the core, oscillating at a frequency ω_0 . The mass of the core is considered to be much bigger than the mass of the electron. For this model, we can write the equation of motion with $\vec{F} = -e\vec{E}$ the force of the electric field on the electron. This gives [3]

$$m_e\ddot{x} + m_e\Gamma_\omega\dot{x} + m_e\omega_0^2x = -e\vec{E}(t), \quad (13)$$

with the solution

$$x(t) = - \left(\frac{e}{m_e} \frac{1}{\omega^2 - \omega_0^2 - i\omega\Gamma_\omega} \right) E(\vec{r}, t). \quad (14)$$

where $\Gamma_\omega = \frac{e^2\omega^2}{6\pi\epsilon_0 m_e c^3}$ is the classical damping rate due to radiative energy loss. The induced dipole moment is equal to $\vec{p} = -e\vec{x}$ [5]. This results in the following relation between induced dipole moment and the electric field

$$\vec{p}(\vec{r}) = \left(\frac{e^2}{m_e} \frac{1}{\omega^2 - \omega_0^2 - i\omega\Gamma_\omega} \right) = \alpha \vec{E}(\vec{r}). \quad (15)$$

Here, α is the complex polarizability of the atom, which is a measure of how easily the light induces a dipole moment. It depends on the light's frequency ω and on the detailed structure of the atom. The real part of the complex polarizability describes the in-phase component of the induced dipole moment with the electric field. It is responsible for dispersive properties of interaction. The imaginary part describes the out of phase component and is responsible for the absorption of radiation, which is later re-emitted as dipole radiation.

In the ODT there is an interaction between the laser light intensity and the dipole moment we just derived. This interaction results in an optical force, making it possible to trap the atoms. Since this force is conservative [3], it can be written as the negative gradient of the potential. This potential is given by [3]

$$U_{\text{dip}} = -\frac{1}{2} \langle \vec{p}(\vec{r}) \vec{E}(\vec{r}) \rangle = -\frac{1}{2\epsilon_0 c} \text{Re}(\alpha) I(\vec{r}) \quad (16)$$

with $I(\vec{r}) = 2\epsilon_0 c |\vec{E}(\vec{r})|^2$, ϵ_0 the dielectric constant and c the speed of light in vacuum. Here $\langle \vec{p}(\vec{r}) \vec{E}(\vec{r}) \rangle$ is the time average over the oscillating terms. The factor 1/2 arises because the dipole is induced and not a permanent one. The dipole force can now be calculated by taking the negative gradient of this potential.

$$F_{\text{dip}}(\vec{r}) = -\nabla U_{\text{dip}}(\vec{r}) = \frac{1}{2\epsilon_0 c} \text{Re}(\alpha) \nabla I(\vec{r}) \quad (17)$$

As mentioned before, the imaginary part of the polarizability is responsible for absorption. The power absorbed by the oscillator is

$$P_{\text{abs}} = \langle \dot{\vec{p}} \cdot \vec{E} \rangle = \frac{\omega}{\epsilon_0 c} \text{Im}(\alpha) I(\vec{r}) \quad (18)$$

This absorbed energy is eventually re-emitted as dipole radiation. The power absorbed can be interpreted as subsequent events in which an atom absorbs and re-emits a photon. We can find the scattering rate by dividing the absorbed power by the energy of a photon

$$\Gamma_{\text{sc}}(\vec{r}) = \frac{P_{\text{abs}}}{\hbar\omega} = \frac{1}{\hbar\epsilon_0 c} \text{Im}(\alpha) I(\vec{r}). \quad (19)$$

With the above equation and the equation for the polarizability we can derive the following expressions

$$U_{\text{dip}}(\vec{r}) = -\frac{3\pi c^2}{2\omega_0^3} \left(\frac{\Gamma}{\omega_0 - \omega} + \frac{\Gamma}{\omega_0 + \omega} \right) I(\vec{r}) \quad (20)$$

$$\Gamma_{\text{sc}}(\vec{r}) = \frac{3\pi c^2}{2\hbar\omega_0^3} \left(\frac{\omega}{\omega_0^3} \right) \left(\frac{\Gamma}{\omega_0 - \omega} + \frac{\Gamma}{\omega_0 + \omega} \right)^2 I(\vec{r}) \quad (21)$$

These equations are often further simplified by taking the rotating wave approximation. In this approximation, rapidly oscillating terms in the Hamiltonian are neglected. The equations simplify to [3]

$$U_{\text{dip}}(\vec{r}) = \frac{3\pi c^2}{2\omega_0^3} \frac{\Gamma}{\delta} I(\vec{r}) \quad (22)$$

$$\Gamma_{\text{sc}}(\vec{r}) = \frac{3\pi c^2}{2\hbar\omega_0^3} \left(\frac{\Gamma}{\delta} \right)^2 I(\vec{r}) \quad (23)$$

However, this approximation is only valid if the laser is detuned relatively close to resonance. So far we have given a mathematical description of the trap potential. The cloud of atoms in the ODT has a certain density distribution that depends on the potential of the trap and the temperature of the atoms. This spatial distribution is discussed in section (2.3).

2.3 Density distribution

The atoms in the ODT have a density distribution that depends on the potential of the trap and the temperature of the atoms. For a finite trap depth ϵ_r , atoms that have an energy ϵ greater than ϵ_r can escape the trap. As high energy atoms are removed, the average energy of the remaining atoms is reduced. The atoms then rethermalize due to elastic collisions to a equilibrium state at a lower temperature. A thermal distribution of the atoms is not possible when the trap depth ϵ_t is finite. This is because an approach to thermal equilibrium is accompanied by loss of atoms due to evaporation [9]. However, if the average energy of the atoms is much smaller than the trap depth $kT \ll \epsilon_r$, then most collisions lead to a redistribution of the energy among the atoms. This leads to a quasi thermal equilibrium. The distribution of the atoms in an evaporating gas is described by a truncated Boltzmann distribution, which is truncated at the trap depth $\epsilon_t = \eta kT$ [9].

$$f(\epsilon) = n_0 \Lambda^3 \exp(-\beta\epsilon) \Theta(\epsilon_t - \epsilon) \quad (24)$$

with

$$\Lambda = \sqrt{\frac{2\pi\hbar^2}{mkT}} \quad (25)$$

the thermal de Broglie wavelength and $\Theta(\epsilon_t - \epsilon)$ the Heaviside step function

$$\Theta(\epsilon_t - \epsilon) = \begin{cases} 0 & \text{if } (\epsilon_t - \epsilon) < 0 \\ 1 & \text{if } (\epsilon_t - \epsilon) \geq 0 \end{cases} \quad (26)$$

The truncation of the Boltzmann distribution is represented in figure (3). Initially we have an atom cloud at a certain initial temperature T . Truncating the tail of this distribution is equivalent to removing the atoms with a high energy.

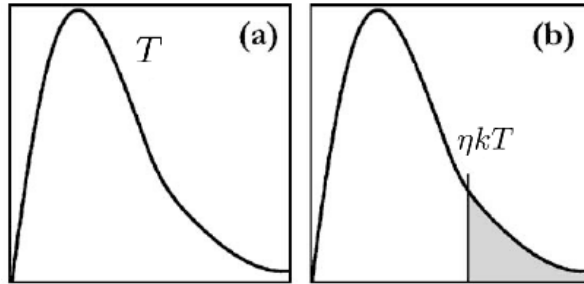


Figure 3: A truncation of the Boltzmann distribution. Figure (a) shows the initial state. In figure (b) the high energy tail of the distribution is removed.

The truncated Boltzmann distribution of equation (24) leads to the phase-space distribution

$$f(\vec{r}, \vec{p}) = n_0 \Lambda^3 \exp[-\beta(U(\vec{r}) + p^2/2m)] \cdot \Theta(\eta kT - U(\vec{r}) - p^2/2m) \quad (27)$$

For large trap depths, truncation effects are small and the Heaviside step function becomes one. The spatial density is then given by [9]

$$n(\vec{r}) = \frac{1}{(2\pi\hbar)^3} \int f(\vec{r}, \vec{p}) d^3\vec{p} \quad (28)$$

After integration over momentum states we obtain the thermal density distribution

$$n(\vec{r}, \beta) = n_0 \exp(-\beta U(\vec{r})) \quad (29)$$

Here, n_0 the density at the centre of the trap, $\beta = (kT)^{-1}$ as usual and $U(x, y, z)$ is the potential. For n_0 to be the density at the centre of the trap, the potential has to be zero at the centre. This equation is valid for an infinite trap depth. However, if the average energy per atom in the trap is much smaller than the trap depth, which is the case in our experiment, then this equation gives a good approximation. This spatial distribution will be used to determine the temperature.

3 Experiment

This section is divided into two parts. First, in section (3.1) the experimental setup is described. In section (3.2) the imaging technique to obtain the density distribution is discussed.

3.1 Experimental setup

The experimental setup essentially consists of a rubidium source and two vacuum chambers that are separated by a differential pumping section. Atoms from the ^{87}Rb source are first trapped in a 2D-MOT. This will give a cigar shaped cloud of atoms, with the length of the cigar in the direction of the 3D-MOT. The atoms are then transported from the 2D-MOT vacuum chamber, through the differential pumping section, into the 3D-MOT vacuum chamber. Here the atoms are captured in the 3D-MOT. The atoms can then be loaded into the optical dipole trap. A top view of the setup is shown in figure (4).

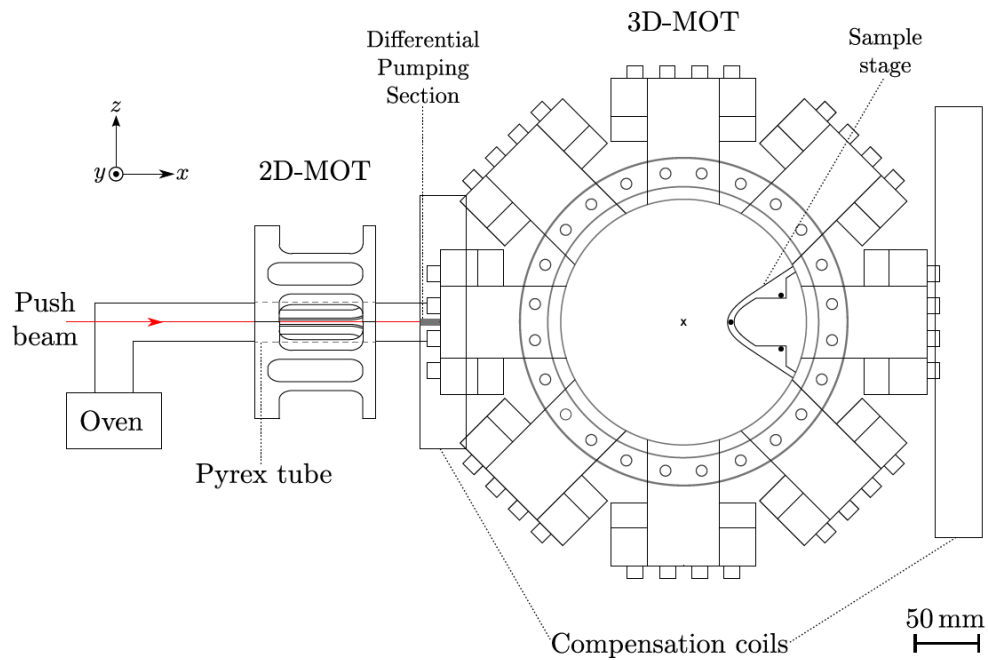


Figure 4: Top view of the setup, image from [7]

3.1.1 Compartments

Rubidium sample

In our experiment we use an ampul of 1g natural rubidium, which consists of 72.17 % ^{87}Rb and 27.83% ^{85}Rb [4]. Only the ^{87}Rb will be cooled. At first, we heated the rubidium above its melting point of 39.3 °C [4] using an oven. However, at the time of the experiment, the oven was turned off, as enough rubidium vapour was in the 2D-MOT chamber.

2D-MOT

The atoms are first loaded in the 2D-MOT. The 2D-MOT has a quadrupole magnetic field in the y, z plane. It is generated by four rectangular coils, each with 81 windings. A current is runs through the coils, which are connected in series. This creates a magnetic field, where the magnetic field is zero along the x - axis. Due to the presence of this magnetic field, the atoms are trapped in a cigar shaped cloud along the x -direction. For the 2D-MOT, we use one laser for cooling and one for re-pumping the atoms.

Differential pumping section

From the 2D-MOT, the atoms are transported to the 3D-MOT through a differential pumping section. This is basically a metal cylinder with a tiny hole in it. Only atoms with a velocity that is aligned with the direction through the hole can travel to the 3D-MOT chamber. This way, a pressure difference between the two chambers is established. The pressure in both chambers is maintained by ion-getter pumps. The atoms are transported from the 2D-MOT to the 3D-MOT chamber by a push beam. This is a laser that is on resonance, which causes the laser to exert a force on the atoms. The push beam is aligned in such a way that it goes from the 2D-MOT chamber, through the differential pumping section, into the 3D-MOT chamber. It 'pushes' the atoms towards the 3D-MOT, so more atoms are loaded.

3D-MOT

The magnetic field of the 3D-MOT is also a quadrupole field and is created by two coils in anti-Helmholtz configuration, each of them having 195 windings. A current of 15.0 A flows through the coils in opposite direction. These coils are also connected in series and are water cooled. The magnetic field created by these coils are strong and influence the magnetic field of the 2D-MOT. To counter this, a compensation coil is placed between the 2D-MOT and the 3D-MOT. This compensation coil has a diameter of 20 cm and has 320 windings. Because this compensation coil will influence the magnetic field of the 3D-MOT, a second compensation coil needs to be placed at the other end. This coil has 320 windings and a diameter of 34 cm. Just as with the 2D-MOT, we need a laser for cooling and one for re-pumping the atoms.

Diode lasers

In the experiment we use five different laser beams locked to different transitions. The transitions of Rubidium can be found in Appendix A. For both the 2D- and 3D-MOT we need a cooling and a re-pump laser. Furthermore, we need another laser that will be split into the reference laser and the push beam. Below is a description of each of the lasers.

- **Cooling**
This laser is used to cool the atoms. It is slightly red detuned with respect to the $F = 2 \rightarrow F' = 3$ transition. We detune the laser in order to cool the atoms using the Doppler shift.
- **Repumping**
When an atom absorbs a photon from one of the cooling lasers, it goes the excited state. Eventually the atom will fall back to the ground state again. In the case of ^{87}Rb , there are two possible ground states the atom can fall into, namely $F = 1$ and $F = 2$. Since the cooling laser is locked on the $F = 1 \rightarrow F' = 3$ transition, atoms that have fallen to the $F = 2$ ground state will not be cooled anymore. Therefore, a re-pump beam is used. This beam is locked at the $F = 2 \rightarrow F' = 3$ transition. If the atom now falls back to the $F = 1$ ground state it can participate in the cooling scheme again.
- **Reference and push**
This laser is locked on atomic resonance. It is used to push the atoms through the differential pumping section into the 3D-MOT chamber. It is also used as a reference laser and in imaging techniques for the optical dipole trap.

3.1.2 Optical dipole trap

The optical dipole trap we use in our experiment is a Gaussian Ytterbium fiber laser with a maximum power of $P = 20$ W and wavelength $\lambda = 1070\text{nm}$. From equations (17) and (20) one can deduce that for a red detuned trap, the potential is negative and the force is directed towards regions of high intensity, i.e. the centre of the trap. We use a large detuning to minimize heating of the atom cloud due to scattering from the dipole trap. Since we use a large detuning, we cannot take the rotating wave approximation. Therefore, the equation we will use for the dipole potential is equation (20). What can also be seen from equations (20) and (21), is that the potential scales with I/δ , while the scattering rate scales as I/δ^2 . In order to keep as many atoms as possible in the trap, the scattering rate needs to be minimized. This is realized by using a large detuning and high intensities. The ODT beam is directed to the atom cloud in the 3D-MOT. The atoms that were in the overlapping volume of the 3D-MOT and the ODT are captured by the ODT. Atoms that are not captured by the ODT will fall away due to gravity. The time the ODT is on after the 3D-MOT is turned

off is the holding time t_{hold} . In the experiment, we will determine the relation between the temperature and the holding time.

3.2 Imaging

The atom density can be determined by absorption imaging. This done by taking images of the atom cloud using a CCD camera. By illuminating the atoms with an on-resonance beam, atoms in the beam's path will cast a shadow on the camera. In the experiment, we use the probe beam as the on-resonance beam. The light intensity on the camera is then a measure of the atom density in the cloud. The transmission of light is given by the Lambert-Beer law, which states

$$T = \frac{I}{I_0} = e^{-\rho_O}. \quad (30)$$

Here, I is the light intensity on the camera and I_0 the initial light intensity, i.e. the intensity of the probe beam in our case. The term ρ_O is the optical column number density, $\rho_O = nl\sigma$, with n the density of absorbing atoms, l the path length through the atom cloud and σ the absorption cross section. We can rewrite equation (30) as

$$\rho_O = -\ln\left(\frac{I}{I_0}\right) \quad (31)$$

When measuring the light intensities, background light has to be taken into account. Therefore three images are taken to calculate the optical density. The first image is of the atom cloud with the probe beam on. This image will give the light intensity after absorption I . A second image is taken without atoms, while the probe beam is still on. This gives the initial intensity I_0 . The third image is taken without atoms and without the probe beam. This will give the background light intensity. Since light from the ODT can scatter into the camera, the ODT is turned off right before the images are taken. To summarize we have the following three images.

image	name	atoms	probe beam
1	I_{atoms}	yes	yes
2	$I_{\text{no atoms}}$	no	yes
3	$I_{\text{background}}$	no	no

Subtracting the background light intensity from both measured intensities, the equation for the optical density (31) can be rewritten as

$$\rho_O = -\ln\left(\frac{I_{\text{atoms}} - I_{\text{background}}}{I_{\text{no atoms}} - I_{\text{background}}}\right). \quad (32)$$

A typical measurement of the optical density is given in figure (5).

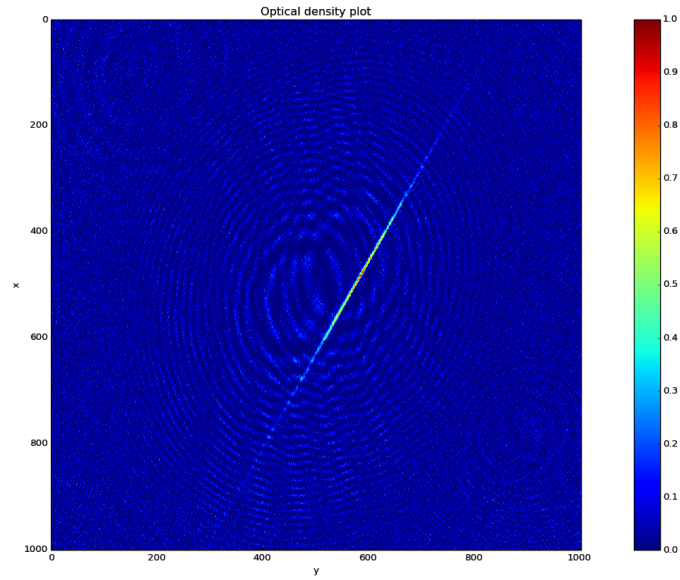


Figure 5: A measurement of the optical density. The yellow region shows a change in light intensity, which indicates that atoms are present in this region. The blue regions correspond to low densities.

Hence, by measuring the light intensities, we can calculate the optical density. This optical density will be used to determine the spatial distribution of the atoms.

4 Results

This chapter is divided into three sections. In section (4.1) the column number density is discussed. In section (4.2) an explanation of the data fitting is given and in section (4.3) the results of the fitting are discussed.

4.1 Column number density

As discussed in section (3.2) we use absorption imaging to determine the optical density. Recall that $\rho_O = nl\sigma$, with n the density of absorbing atoms, l the path length through the atom cloud and σ the absorption cross section. The product nl gives the 2D column number density $n_{2D} = nl$, which is the two-dimensional number density of the atoms. From equation (32) n_{2D} we obtain

$$n_{2D} = -\frac{1}{\sigma} \ln \left(\frac{I_{\text{atoms}} - I_{\text{background}}}{I_{\text{no atoms}} - I_{\text{background}}} \right) \quad (33)$$

Here, σ is the absorption cross section, which is a measure of the probability of an absorption process. It is given by [7]

$$\sigma = \frac{\sigma_0}{1 + s_0} \quad (34)$$

with $\sigma_0 = 3\lambda^2/(2\pi)[4]$ and $s_0 = 0.05[7]$ in our experiment. The images on the camera are magnified. Taking the magnification M into account we obtain

$$n_{2D} = -\frac{M}{\sigma} \ln \left(\frac{I_{\text{atoms}} - I_{\text{background}}}{I_{\text{no atoms}} - I_{\text{background}}} \right) \quad (35)$$

The magnification during our measurements was $M = 0.85$. By applying equation (35) to an image, we can calculate the 2D column number density. In figure (5), the background light intensity is not zero everywhere, as a result of imperfections in the data. To counter this we place a mask around the atom cloud. In the calculations of n_{2D} , we only consider light intensities that are within the mask. This way, the influence of imperfections is minimized. For more accurate data, up to five measurements are taken for each holding time. These five measurements are then averaged. A typical result of an averaged measurement with the mask is shown in figure (6).

In the data fitting we want to work with a linear number density n_{1D} . To obtain n_{1D} , let the z -axis be the long axis of the atom cloud and the x -axis be perpendicular to the z -axis in the plane of the image. Then we obtain n_{1D} by summing the column number densities over the x -axis between the mask at a specific z . This is shown in figure (7).

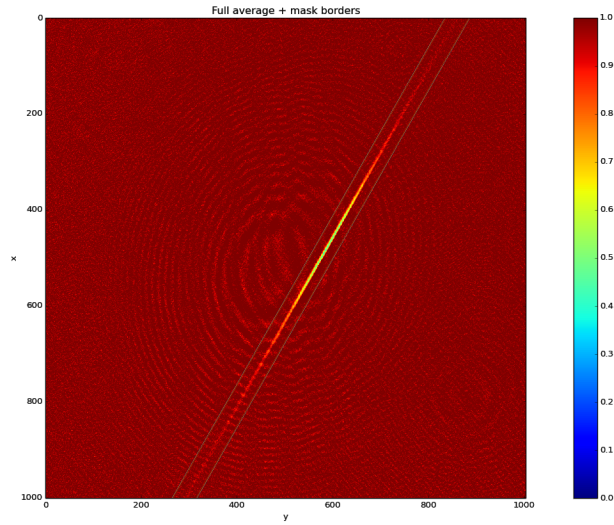


Figure 6: Multiple measurements of the optical density are taken and then averaged. The yellow stripe corresponds to the atom cloud. Mask borders around the atom cloud are shown.

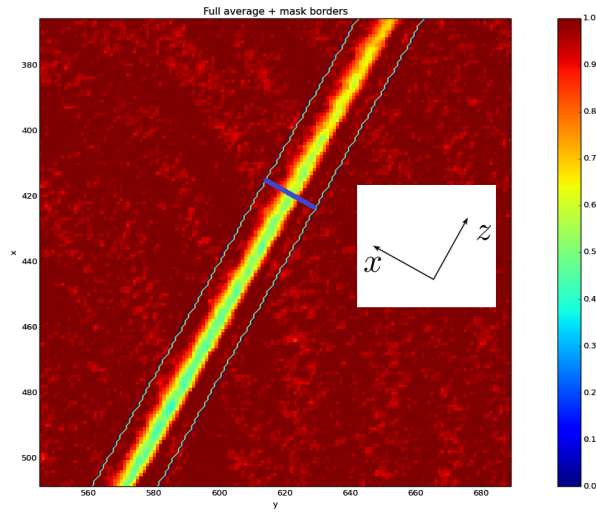


Figure 7: By summing the column number density n_{2D} over the x -axis between the mask borders, we obtain the linear number density n_{1D} . This is indicated as the sum over the blue line

For the linear number density we obtain

$$n_{1D}(z) = \frac{M}{\sigma} \sum_i \rho_O(x_i, z) \quad (36)$$

Hence, by measuring the light intensities we have established a way to calculate the linear number density n_{1D} . We will fit our model of the density distribution to this linear number density. This is discussed in section (4.2).

4.2 Data fitting

The atoms in the ODT have a density distribution that depends on the potential of the trap and the temperature of the atoms. As discussed in section (2.3), our model for the density distribution is given by equation (29)

$$n(\vec{r}, \beta) = n_0 \exp(-\beta U(\vec{r})) \quad (37)$$

For n_0 to be the density at the centre of the trap, the potential has to be zero here. To realize this, we shift the potential up by the trap depth U_0 , which is the absolute value of the potential at the centre. The potential of the trap is given by equation (20).

$$U_{\text{dip}}(\vec{r}) = -\frac{3\pi c^2}{2\omega_0^3} \left(\frac{\Gamma}{\omega_0 - \omega} + \frac{\Gamma}{\omega_0 + \omega} \right) I(\vec{r}) \quad (38)$$

and the intensity distribution of the beam by equation (12).

$$I(r, \omega) = I_0 \exp\left(\frac{-2x^2}{\omega_x^2(z)} + \frac{-2y^2}{\omega_y^2(z)}\right) \quad (39)$$

At the centre, the term in the exponential becomes zero. For the trap depth we then obtain

$$U_0 = \left| -\frac{3\pi c^2}{2\omega_0^3} \left(\frac{\Gamma}{\omega_0 - \omega} + \frac{\Gamma}{\omega_0 + \omega} \right) \frac{2P}{\pi\omega_{x,0}\omega_{y,0}} \right| \quad (40)$$

Note that the value of the potential before shifting is between $-U_0 \leq U_{\text{dip}} \leq 0$. By adding the trap depth to the potential, we obtain

$$U'_{\text{dip}} = U_{\text{dip}} + U_0. \quad (41)$$

This gives $0 \leq U'_{\text{dip}} \leq U_0$, which makes the potential compatible with equation (37). Plugging in U'_{dip} in equation (37) gives

$$n(\vec{r}, \beta) = n_0 \exp(-\beta U'_{\text{dip}}(\vec{r})) \quad (42)$$

with n_0 the desired density at the centre of the trap. This equation gives the three-dimensional number density distribution. To fit this model to our data, we need to rewrite it to a linear number density distribution. This can be done by integrating the density along the x - and y -direction.

$$n_{1\text{D}}(z, \beta) = \int_{-\infty}^{\infty} \int_{-\infty}^{\infty} n(\vec{r}, \beta) dx dy \quad (43)$$

This integral can only be evaluated if the integrand goes to zero for large distances. Taking a look at equation (42) we can see that this is not the case. At large distances from the trap's centre, the density becomes

$$\lim_{r \rightarrow \infty} n(\vec{r}, \beta) = n_0 \exp(-\beta U_0) \quad (44)$$

Therefore we subtract this value from equation (29). By subtracting $n_0 \exp(\beta U_0)$ we obtain

$$n'(\vec{r}, \beta) = n_0 [\exp(-\beta U_{\text{dip}}(\vec{r})) - \exp(-\beta U_0)] \quad (45)$$

We now obtain the linear number density distribution by integrating $n'(\vec{r}, \beta)$, which we will call $n_{1\text{D,fit}}$.

$$n_{1\text{D,fit}}(z, \beta) = \int_{-\infty}^{\infty} \int_{-\infty}^{\infty} n'(\vec{r}, \beta) dx dy \quad (46)$$

To determine the temperature, we will fit $n_{1\text{D,fit}}$ to our data. This is discussed in section (4.3).

4.3 Temperature

Before we fit the model to our data, let us first discuss the dynamics of the atoms in the ODT. The collisional dynamics in the atom cloud are typically described by the change in atom number N and total energy E , as was originally suggested by Hess [11]. Here, we assume that the ratio of the trap depth ϵ_r to kT is large. The atom number and energy evolution in the trap can be modelled by [8]

$$\dot{N} = \dot{N}_{ev} + \dot{N}_\theta + \dot{N}_{1B} + \dot{N}_{3B} \quad (47)$$

$$\dot{E} = \dot{E}_{ev} + \dot{E}_\theta + \dot{E}_{1B} + \dot{E}_{3B} \quad (48)$$

In these equations, terms with the subscript "ev" account for atom number and energy loss due to evaporation, subscript " θ " for changes in the shape of the trap and "1B" and "3B" for one- and three-body collisions. In our experiment, we do not change the shape of the trap. Therefore atom and energy loss due to the changing of the trap, \dot{N}_θ and \dot{E}_θ are neglected. The different terms in these equations are now discussed.

Evaporation

In the trap, elastic collisions produce atoms with an energy higher than $\epsilon_r = \eta kT$. The production rate of these high energy atoms is equal to the number of atoms with energy higher than ηkT divided by their collision time. As stated in section (2.3), the distribution in the trap can be described by a truncated Boltzmann distribution that is truncated at the trap depth. If η is large, then the rate at which atoms evaporate out of the trap is identical to the rate at which high energy atoms are produced in the untruncated distribution. The velocity of atoms with energy $\epsilon = \eta kT$ is $\sqrt{2\eta kT/m} = \sqrt{\pi\eta}\bar{v}/2$, with \bar{v} the average thermal velocity. For large trap depths, the fraction of atoms with energy larger than the trap depth approaches $2e^{-\eta}\sqrt{\eta/\pi}$. The rate of evaporating atoms is [10]

$$\dot{N} = -Nn_0\sigma\bar{v}\eta e^{-\eta} = \frac{-N}{\tau_{ev}} \quad (49)$$

with τ_{ev} the time constant for evaporation. Thus, the loss in atom number is proportional to current atom number. The average energy removed by each evaporated atom is $(\eta + \kappa)kT$ where $\kappa \simeq (\eta - 5)/(\eta - 4)$ [8].

One- and three-body collisions

For the one- and three-body collisions we have [8]

$$\dot{N}_{1B} + \dot{N}_{3B} = -\Gamma_{1B} \int n(\vec{r}) d^3\vec{r} - L_{3B} \int n(\vec{r})^3 d^3\vec{r} \quad (50)$$

$$= -\Gamma_{1B}N - \Gamma_{3B}N \quad (51)$$

$$\dot{E}_{1B} + \dot{E}_{3B} = -\Gamma_{1B} \int e(\vec{r}) d^3\vec{r} - L_{3B} \int n(\vec{r})^2 e(\vec{r}) d^3\vec{r} \quad (52)$$

$$= -\Gamma_{1B}E - \Gamma_{3B} \frac{2}{3}E \quad (53)$$

Here, $\Gamma_{3B} = L_{3B}n_0^2/3\sqrt{3}$, $L_{3B} = 4.3(\pm 1.8) \times 10^{-29} \text{ cm}^6 \text{ s}^{-1}$ for ^{87}Rb [8]. The Γ_{1B} is mainly due to background collisions and therefore depends on the conditions of the vacuum chamber. With these results, we can rewrite equations (47) and (48) to

$$\dot{E} = -N\Gamma_{ev}(\eta + \kappa)kT - \Gamma_{1B}E - \Gamma_{3B} \frac{2}{3}E \quad (54)$$

$$\dot{N} = -(\Gamma_{ev} + \Gamma_{1B} + \Gamma_{3B})N \quad (55)$$

We see that both the rate of the energy loss and the loss of number of atoms depends on the current number of atoms N . Therefore, we expect the temperature to drop faster with higher atom numbers. Also, since the atom number decreases due to the evaporation, the rate at which the temperature drops is expected to decrease.

By fitting the model to our data we obtain the values of β for different holding times t_{hold} . Once we have found β the temperature is obtained by $T = (k\beta)^{-1}$. In figures (8) and (9) the temperature is plotted against the holding time. In figure (8) we started with $N \simeq 275\,000$ and in (9) $N \simeq 125\,000$ atoms. Based on the results of equations (54) and (55), we would expect that the temperature will drop faster in figure (8) due to the higher atom number. Since the atom number is higher for short holding times, the rate at which the temperature drops is higher for short holding times. This can be seen in the figures, as the rate at which the temperature decreases is highest for holding times between 100 and 500 ms. After that, the decrease in temperature stabilizes.

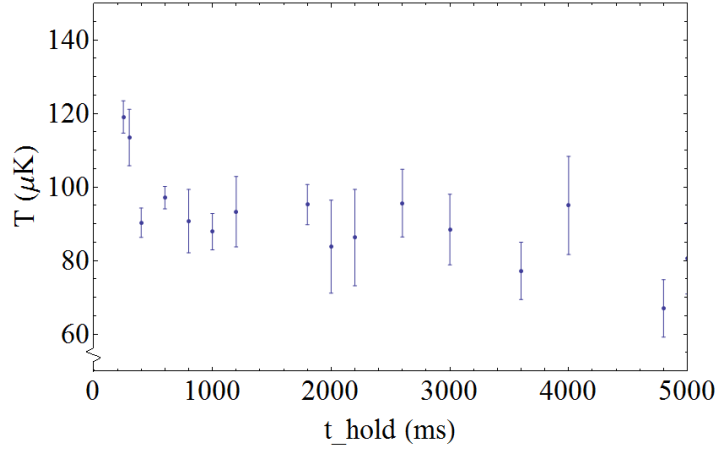


Figure 8: Temperature T of the atom cloud plotted against the holding time t_{hold} . Here we started out with $N \simeq 275000$ atoms.

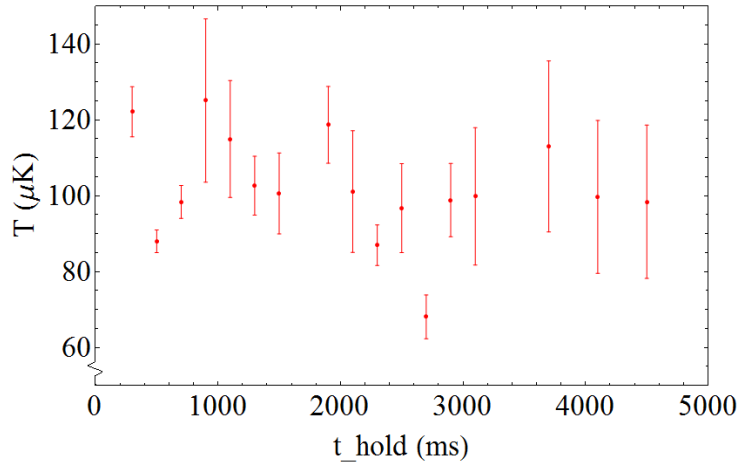


Figure 9: Temperature T of the atom cloud plotted against the holding time t_{hold} . Here we started out with $N \simeq 125000$ atoms.

5 Conclusion

We have successfully established a way to determine the temperature in the optical dipole trap. The temperature evolution of two different runs was measured, which differed in atom number. In one of the runs, we started out with a higher atom number than the other one. In both of the runs, we discovered a decrease in temperature. One possible explanation for the temperature drop is the evaporation of atoms, due to collisional processes in the optical dipole trap. When atoms with a higher energy than the average energy escape, the atom cloud rethermalizes to a lower temperature. This causes the temperature to decrease. As is concluded in the results, the rate at which the temperature decreases depends on the number of atoms in the trap. A higher number of atoms causes the temperature to drop at a faster rate. We concluded that the temperature decrease was more evident in the run with a higher atom number. We concluded that in both runs, the rate at which the temperature decreases is higher for shorter holding times. For larger holding times, when the number of atoms was lower, the drop rate of the temperature stabilized.

Since the change in temperature is largest for shorter holding times, it would be interesting to focus more on these points. However, in our experiment it was not possible to do measurements at shorter holding times. At these shorter holding times, the presence of the MOT still influenced the measurements. One could imagine an experiment where it is still possible to perform temperature measurements at these shorter holding times. It is possible to load the trap with a deep trap depth and let the system thermalize. When the trap depth is suddenly lowered, atoms will evaporate out of the trap. In this situation, it is then possible to perform temperature measurements at short holding times.

6 Acknowledgements

I would like to thank Dries van Oosten, Ole Mussman and Sandy Pratama for supervising my work. Even though there was some bad luck with the experimental setup, they were very helpful in providing a good alternative. Special thanks go out to Sandy, without your help, my thesis wouldn't be what it is today. I also would like to thank Sebastiaan Greveling and Maarten Dobbelaar for the relaxing lunches in between.

7 A Rubidium hyperfine structure

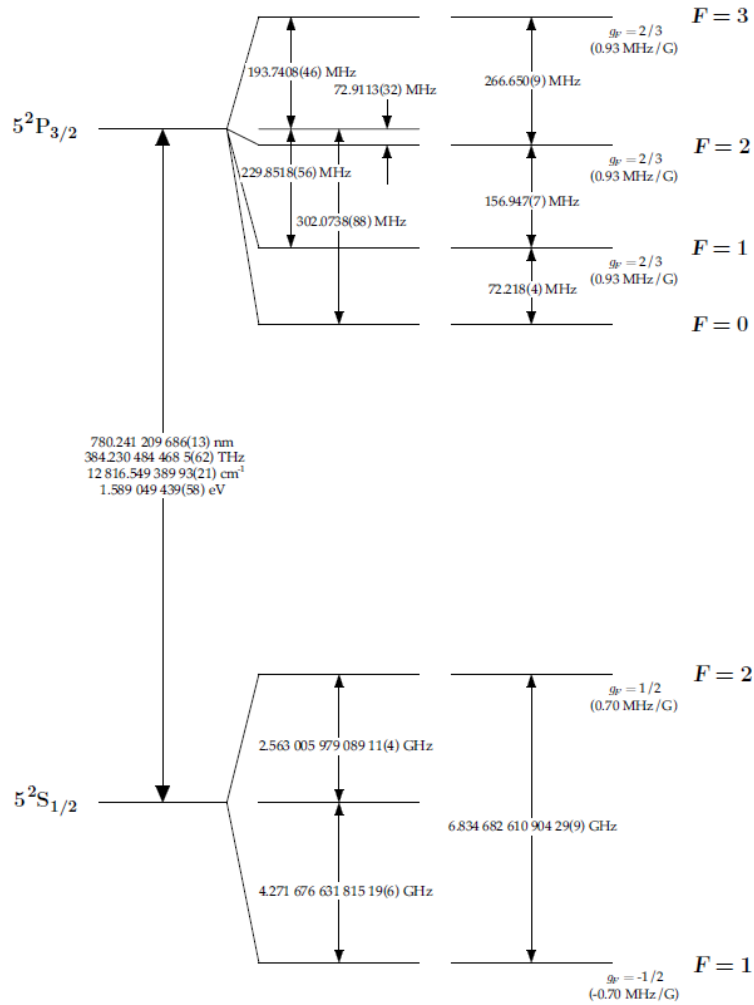


Figure 10: Rb transition hyperfine structure, taken from [4]

References

- [1] Metcalf, H.J., van der Straten, P., *Laser Cooling and Trapping*, Springer-Verlag New York, Inc (1999)
- [2] H.J. Metcalf and P. van der Straten, P. *Laser Cooling and trapping of neutral atoms paper*, Physics Reports 244, pp. 203-286 (1994)
- [3] Grimm, R., Weidemüller, M., Ovchinnikov, *Optical Dipole Traps for Neutral Atoms*, Advances in Atomic, Molecular and Optical Physics **vol. 42**, pp.95-170 (2000)
- [4] Steck, D.A. *Rubidium 87 D-line data* (2001)
- [5] Griffiths, D.J. *Introduction to electrodynamics*, Pearson Education, Inc., 3rd ed., (1999)
- [6] Silvast, W.T. *Laser Fundamentals*, Cambridge University Press, 2nd ed. (2004)
- [7] Greveling, S. An Optical Conveyor for Light-Atom Interaction, Master thesis, Utrecht University, (2013)
- [8] Olson, A.J., Niffenegger, R.J., Chen, Y.P., *Optimizing the efficiency of evaporative cooling in optical dipole traps*, Phys. Rev. A **vol. 87**, p. 053613 (2013)
- [9] Luiten, O.J., Reynolds, M.W., Walraven, J.T.M., *Kinetic theory of the evaporative cooling of a trapped gas*, Phys. Rev. A **vol. 52**, pp. 381-389
- [10] Ketterle, W., van Druten, N.J. *Evaporative Cooling of Trapped Atoms*, Advances in Atomic, Molecular and Optical Physics **vol. 37** (1996)
- [11] Hess, H.F., *Evaporative cooling of magnetically trapped and compressed spin-polarized hydrogen*, Phys. Rev. B **vol.34**, pp. 3476-3479 (1986)